Electronic Supplementary Material (ESI) for Physical Chemistry Chemical Physics.

Supplementary Information

Computational elucidation of aging time effect on zeolite synthesis selectivity in the presence of water and a diquaternary ammonium iodide

Bahram Ghanbari[a*], Fatemeh Kazemi Zangeneh[a], German Sastre[b], Maryam Moeinian[a], Sina Marhabaie[c], Zahra Taheri Rizi[d]

[a] Department of Chemistry, Sharif University of Technology, PO Box 11155-3516, Tehran, Iran

[b] Instituto de Tecnologia Quimica U.P.V.−C.S.I.C., Universidad Politecnica de Valencia, Avenida Los Naranjos s/n, 46022 Valencia, Spain

[c] Laboratoire des biomolécules, LBM, Département de chimie, École normale supérieure, PSL University, Sorbonne Université, CNRS, 75005 Paris, France

[d] Research Institute of Petroleum Industry, West Blvd. of Azadi Complex, Tehran 1485733111, IRAN

Corresponding author: Tel. +98 21 66165307, Fax +98 21 66005718

E-mail: ghanbari@sharif.edu

Index

S1. Physico-chemical characterization.

^{1}H and ^{13}C NMR, CHN micro analysis, XRD, FT-IR, FE-SEM, TGA/DTG, Raman and solid state NMR techniques were used to characterize the TMDP as well as the occluded zeolites with or without TMDP. Details of the instruments employed are given here:

Raman spectroscopy. Raman spectrum was recorded on Teksan Spectroscopy (Model: Takram P50C0R10) in the region 100-4400 ± 0.6 (cm^{-1}).

CHN micro analyses. The elemental microanalyses were determined on a Truspec CHNS-Com Leco instrument (USA).

^{1}H and ^{13}C NMR. ^{1}H and ^{13}C NMR spectra (500 MHz) were also obtained in D_2O for the soluble samples on a Bruker-ARX500 instrument at ambient temperature.

X-ray diffraction (XRD). The powder X-ray diffraction (XRD) patterns of the zeolites were determined on a D8 Advance Bruker X-ray diffractometer using Cu K_α radiation (λ = 1.5406 Å) source operating at 40 kV and 30 mA. The spectra were carried out in a scanning range of 2θ=5°-80° at room temperature.

Thermogravimetric analysis (TGA). Thermal gravimetric analysis (TGA) was executed by applying a SDT Q600 V20.9 Build 20 TGA instrument. The samples were heated from 30–800 °C under air flow (15 L min^{-1}) at a rate of 15°C min^{-1}.

^{1}H MAS and ^{13}C CP-MAS NMR spectra. ^{1}H MAS and ^{13}C CP-MAS NMR (Magic-Angle Spinning Nuclear Magnetic Resonance) spectra were recorded using an 800 MHz Bruker spectrometer working at 800.29 MHz and 201.25 MHz (for ^{1}H and ^{13}C respectively) at room temperature, employing a 3.2 mm probe. The powder samples were filled in rotors and rotated at the magic angle spinning (MAS) at 24.00kHz.

Field Emission Scanning electron microscopy (FE-SEM). FE-SEM images were acquired on a TESCANMIRA3-LMU scanning electron microscope, using a potential difference of 15 kV. The zeolite crystals were deposited on a silicon wafer by dispersion, whereby the samples were successively enclosed with a gold film.

Fourier transforms infrared (FT-IR) spectroscopy. Fourier Transform Infrared (FT-IR) spectra was measured by a RXI-Perkin-Elmer spectrophotometer at room temperature by using KBr pellets, having the resolution of 4 cm^{-1} at the mid-infrared range of 400-4000 cm^{-1}. Fig. S1 displays FT-IR spectra of the samples in the range 400-4000 cm^{-1}.

Mass spectroscopy (MS). The mass spectra of the compounds were measured on an Agilent Technology (HP)-5973 mass spectrometer.

S2. Fourier transforms infrared (FT-IR) spectroscopy.

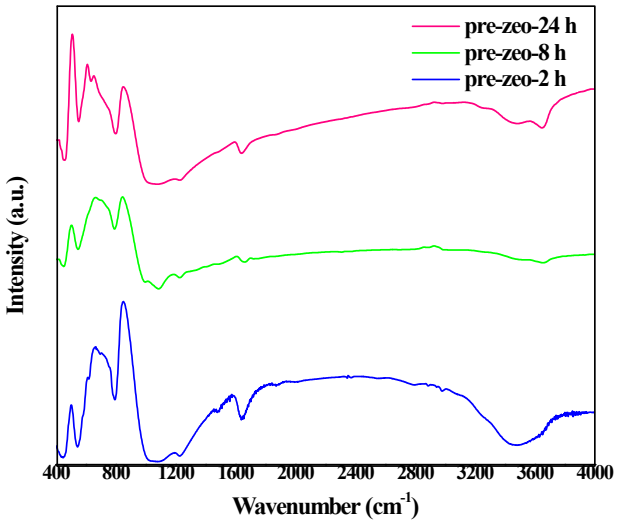

Fig. S1 FT-IR spectra of **pre-zeo-2 h**, **pre-zeo-8 h** and **pre-zeo-24 h** samples.

In the FT-IR spectra of **pre-zeo-2 h** and **pre-zeo-8 h**, the broad bands in 3450 and 1370 cm^{-1} were assigned to bridging and interacting OH groups in zeolite, respectively; whilst the other recorded band in 1640 cm^{-1} can be attributed to physically absorbed water.

The bending vibrations of the primary $SiO_{4/2}$ and $AlO_{4/2}$ tetrahedra in zeolite can be also assigned by the characteristic band at ~450 cm^{-1} in the spectra, whereas the corresponding main group frequencies appeared in the 500-650 cm^{-1} range.[1]

The recorded spectra for **pre-zeo-8 h** and **pre-zeo-24 h** in Fig. S1 displayed typical vibrational bands at 1225 cm^{-1} for asymmetric stretching; 1050 cm^{-1} for symmetric stretching; 800 and 720 cm^{-1} for and 450 cm^{-1} for T–O bending.[2]

S3. Raman spectroscopy.

Fig. S2 illustrates the Raman spectra of **pre-zeo-8 h** and **pre-zeo-24 h** in 600-1600 cm^{-1} region with the Raman spectra of TMDP in aqueous solution.

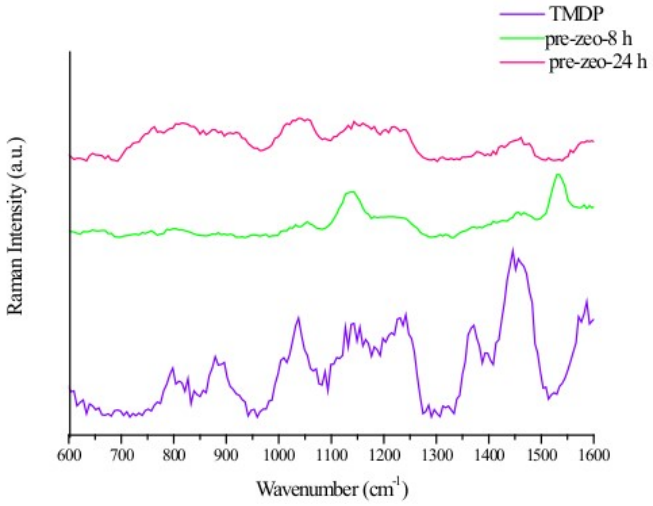

Fig. S2 Raman spectra of **pre-zeo-8 h**, **pre-zeo-24 h** and TMDP in 600-1600 cm^{-1}. The spectrum of **pre-zeo-2 h** is omitted due to the low intensity of bands.

As seen in Fig. S2, the Raman features of **pre-zeo-8 h** and **pre-zeo-24 h** are significantly different from TMDP in aqueous solution, indicating the occlusion of TMDP within the zeolite pores, hindering its vibrational modes. Comparing the corresponding asymmetric deformation and CH_3 stretching modes at 1450-1500 cm^{-1} and 2750-3000 cm^{-1} respectively; in free TMDP and those trapped in **pre-zeo-8 h** and **pre-zeo-24 h**, one can conclude that the CH_3 groups of the guest OSDAs interact with the channel/pore of the zeolite framework. Further, Fig. S2 shows that also another vibrational band changes at 750-950 cm^{-1}, in terms of both their frequencies and intensities, assigned to the C–N stretching vibration mode of the occluded TMDA. These changes are more pronounced than those described in previous reports.[3,4]

S4. ^{13}C MAS NMR spectra of zeolite precursors.

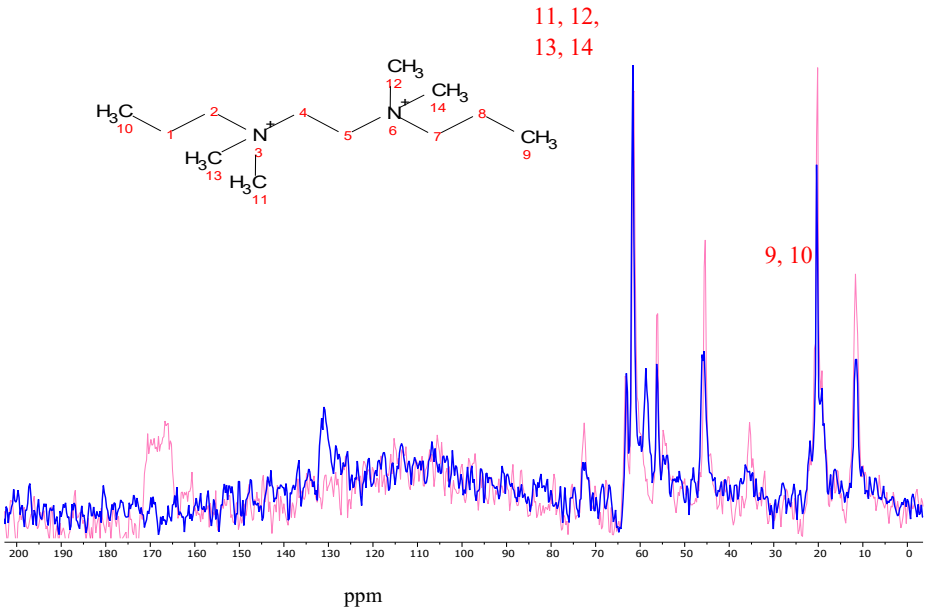

Fig. S3 Overlay of ^{13}C MAS NMR spectra of **pre-zeo-8 h** (blue) and **pre-zeo-24 h** (red) zeolites containing occluded TMDP.

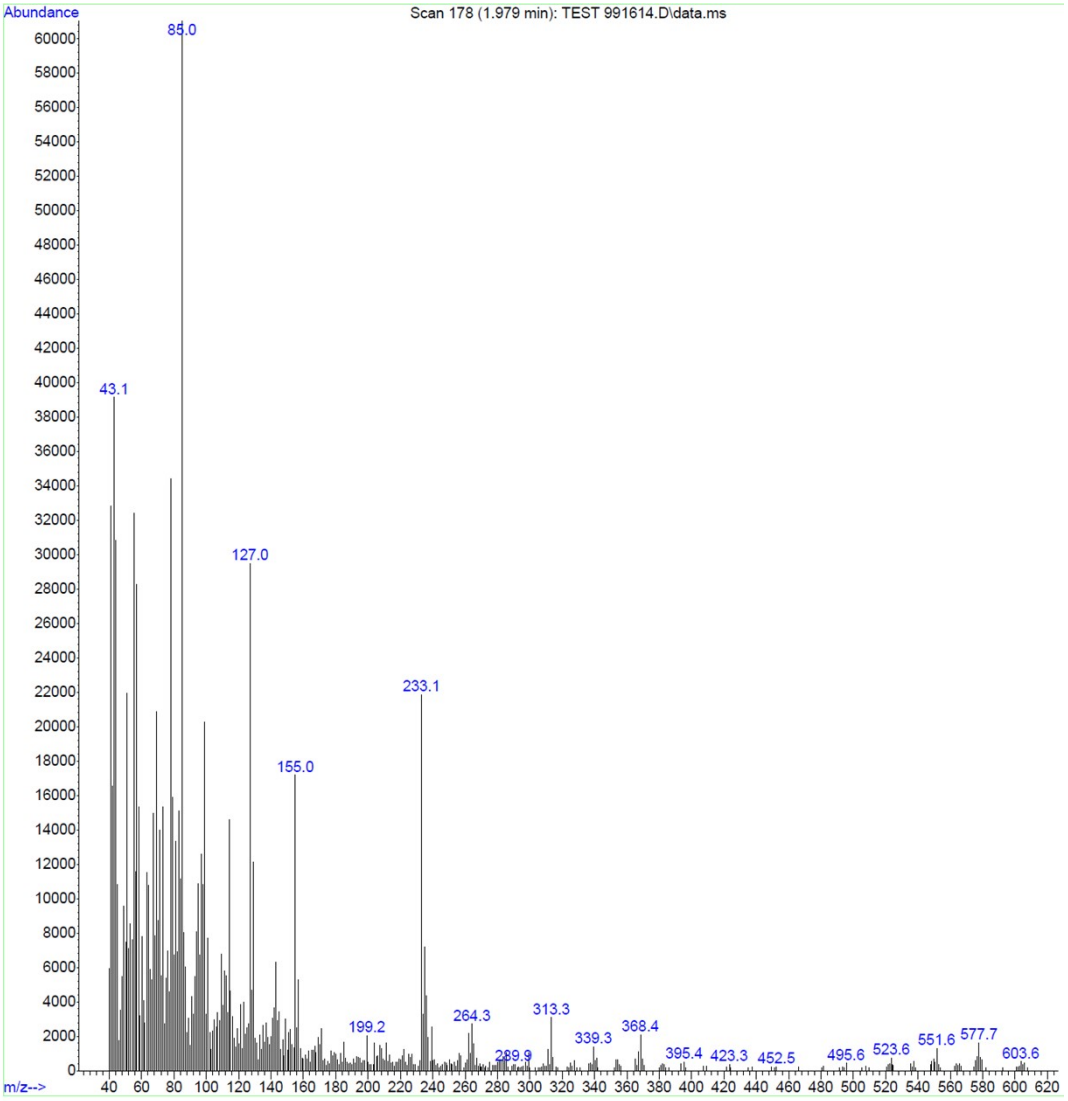

Fig. S4 The mass spectrum of the sample retrieved by HF digestion of **pre-zeo-2 h**

Table S1. The observed and calculated mass numbers measured for the product of **pre-zeo 2 h** digestion by HF

m/z	Abundance		
85	60992	85/2	[(M'-2HI)/2]-H	☑
86/1	8031	86/2	[(M'-2I)/2]-H	☑
87	6032	87/2	(M'-2I)/2	☑
99/1	20280	99/2	[(M-2HI)/2]-H	☑
100	3288	100/2	[(M-2I)/2]-H	☑
101	7729	101/2	(M-2I)/2	☑
149/1	3024	149/6	[(M'-I)/2]-H	☒
150/1	1215	150/1	[(M'-HI)/2]	☑
151/1	2199	150/6	(M'-I)/2	☒
163/1	1126	163/6	[(M-I)/2]-H	☒
164/1	524	164/2	[(M-HI)/2]	☑
165/1	1206	164/6	(M-I)/2	☒
172/1	584	172/3	M'-2HI	☑
173/1	662	173/3	M'-HI-I	☑
174/1	298	174/3	M'-2I	☑
200	506	200/4	M-2HI	☒
201/1	339	201/4	M-HI-I	☑
201/9	343	202/4	M-2I	☒
212	549	212/1	(M'/2)-2H	☑
213/2	934	213/1	(M'/2)-H	☑
214/1	430	214/1	M'/2	☑
226/1	765	226/1	(M/2)-2H	☑
227/1	979	227/1	(M/2)-H	☑
228/1	337	228/1	M/2	☑
299/3	1062	299/2	M'-HI-H	☑
300/1	170	300/2	M'-HI	☑
303/3	150	301/2	M'-I	☒
327/3	614	327/3	M-HI-H	☑
329/3	189	329/3	M-I	☑
421/4	219	426/1	M'-2H	☒
423/3	356	427/1	M'-H	☒
424/2	165	428/1	M'	☒
449/3	227	454/2	M-2H	☒
451/5	158	455/2	M-H	☒
452/5	232	456/2	M	☒

S5. Computational details

The geometry optimizations were performed using the GULP code,[5,6] employing the Ewald method for summation of the long range Coulombic interactions, and direct summation of the short range interactions with a cut off distance of 12 Å. The BFGS (Broyden-Fletcher-Goldfarb-Shanno)[7-10] technique was employed as the cell minimization scheme with a convergence criterion of a gradient norm below 0.001 eV/Å. Full optimizations of all the atoms of the system (zeolite + SDA + water) have been performed, and also the unit cell parameters were optimized. SDA molecules are: TMDP ($C_{12}N_2H_{30}$), DMDP ($C_{10}N_2H_{24}$), or Imidaz ($C_{10}N_2H_{22}$). For the organic SDAs, the charge distribution was obtained by means of a charge equilibration method.[11] Both all-silica and Si/Al zeolites were considered.

Another aspect in our methodology is the contributions to the total energy of the different terms. Some previous studies taking into account the thermodynamic aspects of the synthesis of zeolites as well as a rough estimation of some aspects related to the kinetics have been presented[12] Expanding from previous studies, here we consider the total energy due to all constituents of the system as:

$$E_{\text{total}} = E_{\text{zeo'}} + E_{\text{zeo' - water}} + E_{\text{zeo' - }SDA} + E_{\text{water - }SDA} + E_{\text{water - water}} + E_{SDA\text{ - }SDA} + E_{\text{water}} + E_{SDA} \quad (1)$$

In this equation, the notation *zeo'* refers to the geometry of the final system where the zeolite energy includes the deformation due to the effect of loading. Moreover, all other geometries (for water and OSDA) were considered in the optimized configuration. These energetic terms contain three contributions: intramolecular (bonding, van der Waals and electrostatic), intermolecular-1 (van der Waals), and intermolecular-2 (electrostatic), using the forcefield in previous studies[13-15].

GULP allows to activate and deactivate each contributions by making, after obtaining the final optimized geometry, a single point calculation including the selected term. An exception is the case of the electrostatic, where all the atoms in the system are always calculated and where the requirement of electroneutrality should be strictly met. The very useful keywords 'molmec' and 'molecule' allow to calculate respectively the electrostatic 'inter+intra' or 'inter' contributions, giving a large flexibility to know the different terms. The 'molecule' keyword, however, cannot be used for 'periodic molecules', hence only for water/OSDA systems, but still this is of great help. A careful definition of energetic terms is recommended to avoid duplicates and ensure that the final summation corresponds to the total energy.

Subtraction of separate calculations (in the all-silica system) allows to isolate the desired electrostatic contributions. For instance, in the zeo-TMDP system, the electrostatic energy, that we may call 'Energy1', includes: self-electrostatic(zeo)+electrostatic(zeo-TMDP)+electrostatic(TMDP-TMDP). Two separate calculations of: (i) zeo, and (ii) TMDP, allow to obtain: electrostatic(zeo) (Energy2), and electrostatic(TMDP-TMDP) (Energy3). Hence, the electrostatic zeo-TMDP is: Energy1-Energy2-Energy3. The relevant terms are included in Table S2. The energetic terms that played a more important role were the intermolecular van der Waals: zeo-OSDA, zeo-water, water-water, and water-OSDA. Each system (MFI, MOR) contains:

2 TMDP molecules and 42 water molecules (for water weight loss 11.0%)

TMDP+Imidaz and 26 water molecules (for water weight loss 8.0% and 7.0%)

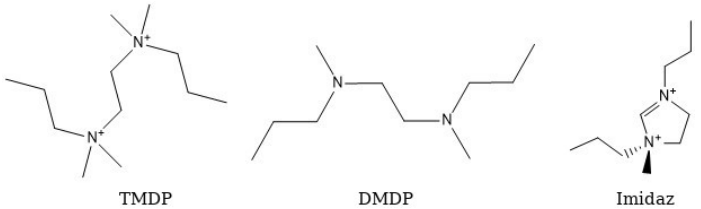

Figure S5. OSDAs considered in the calculations.

The results are divided in two types of calculations, without aluminum –i.e. pure silica- (Table S2, below) and with aluminum (main article, Table 4). The calculation below (using all-silica zeolite) imply that the SDA molecules, although containing atomic charges different from zero, have overall neutral charge, as well as the zeolite, also neutral. This allows to fully apply the energetic decomposition above since each term must contain a neutral entity because charged periodic systems do not have an energy defined.

Table S2. Different energetic contributions (kcal/mol) of systems zeo+SDA+water. SDA loading is 2 molecules per u.c. (96 SiO_2), as follows: TMDP+TMDP and TMDP+Imidaz, each one of them with the water content estimated from section S6. The system with larger (42) water content corresponds to the pre-zeo-2h sample, and that with smaller water (26) is representative of samples pre-zeo-8h and pre-zeo-24h. Unit cells are 1×1×1 for MFI and 1×1×2 for MOR, both containing 96 SiO_2.

Type of interaction	**pre-zeo-2h**		**pre-zeo-8h, pre-zeo-24h**	
	TMDP+TMDP (42 water)		**TMDP+Imidaz (26 water)**	
	MFI	**MOR**	**MFI**	**MOR**
Zeo-water(vdw) (1)	-75.1	-80.8	-39.3	-79.9
SDA-water(vdw) (2)	-9.6	-12.2	-9.0	-6.9
Zeo-SDA(vdw) (3)	-56.1	-55.4	-34.9	-38.3
water-water(vdw) (4)	-18.6	-8.4	-7.4	-5.6
zeo+SDA+w+SDA-SDA+Coul(1-4)	-89631.6	-89619.0	-89568.2	-89575.3
Total*	**-89791.0**	**-89775.8**	**-89658.8**	**-89706.0**

*zeo-w(inter)+w-w(inter)+SDA-w(inter)+SDA-SDA(inter)+zeo-SDA(inter)+zeo(intra)+SDA(intra)+w(intra)

Total energy calculations show that MFI is the most stable zeolite at large water content (corresponding to the pre-zeo-2h sample), whilst MOR is the most stable zeolite at the smaller water content (pre-zeo-8h and pre-zeo-24h), in agreement with our experimental observation of the MFI → MOR phase transformation at higher aging times.

The larger stability of MOR at smaller water content (26) is mainly due to the large zeo-water stabilization (-79.9 kcal/mol in MOR versus -39.3 kcal/mol in MFI), that is favoured by the interaction of water with the small pockets of the MOR framework. When the water content increases (42), the tendency of zeo-water stabilization becomes more similar (-75.1 and -80.8 kcal/mol in MFI and MOR), due to less favourable filling of water on the large cavity of MOR, whilst water finds a more size-homogeneous micropore and increasing water molecules do still interact favourably with the zeolite. Obviously, the water filling arrangements are different, and can be dynamically changing the location, and it is not easy to rationalize the results. The fact that we have considered two different OSDA arrangements was owing to simulating the thermal decomposition of TMDP to give Imidaz as the aging time increases. This is also an important factor since the locations of the OSDAs are slightly different and this also influences the water location.

S6. OSDA and water content of MFI and MOR.

We assume that unit cells of 96(SiO_2) contain either two TMDP ($C_{12}N_2H_{30}$) molecules or a mixture of TMDP+DMDP($C_{10}N_2H_{24}$), or TMDP+Imidaz($C_{10}N_2H_{22}$). Neglecting the mass of surface silanols (which will not contribute appreciably to the measured %H), and calling 'w' the number of water molecules, we have:

mass of 96(SiO_2)=96×60 ; mass of SDA: TMDP=n_1×202; DMDP=n_2×172; Imidaz=n_3×170;

mass of water = 18×w; H mass = n_1×30+n_2×24+n_3×22+2×w; C mass = n_1×144+n_2×120+n_3×120;

Total mass = 96×60 + n_1×202 + n_2×172 + n_3×170 + 18×w

From the water loss at 300-500 ºC (physically adsorbed water), we obtain:

$18\times w/(5760+n_1\times 202+n_2\times 172+n_3\times 170+18\times w)$ = water weight loss (0.110, 0.080, 0.070) (1)

Using equation (1), different pairs of OSDA-water contents were calculated (Table S3). From the fact (from calculations) that it is impossible to have loadings larger than 40 molecules when OSDA content is larger than 2 molecules per unit cell (96 SiO_2), it follows that 2 molecules are the only possibility (Figures S6 and S7).

For the pre-zeo-2h sample (water weight loss = 11.0%), it is clear that TMDP shows integrity and hence 2 TMPD molecules per unit cell is clearly the best option, with the following equation:

$18\times w/(5760+2\times 202+18\times w) = 0.110$ (2)

Solving equation (2), the corresponding water content is 42 (Table S3), which gives 2.1%, 4.2% and 16.8% for the hydrogen, carbon and total weight losses respectively, which compare very accurately with the experimental results of 2.28%, 4.18% (Table 3), and not so well with the experimental weight loss of 12.3% (Table 2). The latter is due to the incertitude in deciding the temperature at which water removal is complete from the TGA experiments (Figure 3). We have chosen a typical range of 300-500 °C, but we have also made calculations with 150 and 200 °C and the results are qualitatively similar. It is quite possible that the OSDA partial decomposition is simultaneous to the water loss and regardless the temperature chosen the weight loss is not only water. Hence this is the reason of the disagreement of the calculated and experimental total weight loss.

The fit for the other samples (**pre-zeo-8h** and **pre-zeo-24h**) is not easy. According to section 3.3, TMDP decomposition leads to formation of DMDP and Imidaz, and hence we have considered TMDP+DMDP and TMDP+Imidaz (50%+50%, thus 1 molecule of each SDA). The equations are:

$18\times w/(5760+202+172+18\times w) = 0.080$ (3a)

$18\times w/(5760+202+170+18\times w) = 0.080$ (3b)

$18\times w/(5760+202+172+18\times w) = 0.070$ (4a)

$18\times w/(5760+202+170+18\times w) = 0.070$ (4b)

This gives 30 water molecules for water weight loss = 8.0% (**pre-zeo-8h** sample) and 26 water molecules for water weight loss = 7.0% (pre-zeo-24h sample) respectively (Table S3). We choose the value of 26 water molecules for the system with TMDP+Imidaz.

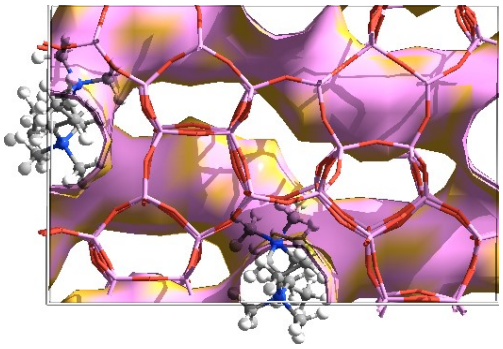

Figure S6. MFI zeolite with 2 molecules of TMDP.

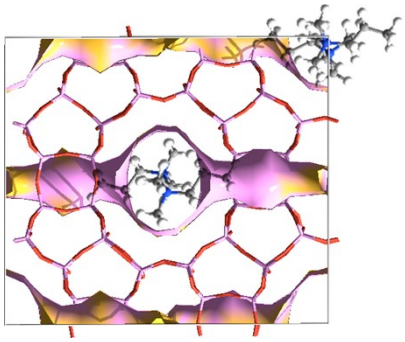

Figure S7. MOR zeolite with 2 molecules of TMDP.

Table S3. Different possibilities to fit the calculated water and OSDA content with the experimental total weight loss (12.3, 11.9, 11.1%, Table 2) as well as carbon and hydrogen weight loss (Table 3), by using the experimental water weight loss (11.0, 8.0, 7.0%, Table 2). Using equations 1-4 above, OSDA contents were tested between 2 and 4. Selection of OSDA and water content explained in the main text.

water weight loss	TMDP content 2	TMDP content 3	TMDP content 4	TMDP content 2	TMDP content 3	TMDP content 4	TMDP content 2	TMDP content 3	TMDP content 4	TMDP content 2	TMDP content 3	TMDP content 4
	water content			%H			%C			%TMDP		
0.110	42	44	45	2.1	2.5	2.8	4.2	6.0	7.8	5.8	8.5	10.9
0.080	30	31	32	1.8	2.2	2.6	4.3	6.2	8.1	6.0	8.8	11.3
0.070	26	27	27	1.7	2.1	2.5	4.3	6.3	8.2	6.1	8.9	11.4

water weight loss	Imidaz content 2	Imidaz content 3	Imidaz content 4	Imidaz content 2	Imidaz content 3	Imidaz content 4	Imidaz content 2	Imidaz content 3	Imidaz content 4	Imidaz content 2	Imidaz content 3	Imidaz content 4
	water content			%H			%C			%Imid		
0.110	42	43	44	1.9	2.2	2.4	3.5	5.1	6.6	5.0	7.2	9.4
0.080	29	30	31	1.6	1.9	2.1	3.6	5.3	6.9	5.1	7.5	9.7
0.070	26	26	27	1.4	1.8	2.0	3.7	5.3	6.9	5.2	7.6	9.8

water weight loss	OSDA content 2	OSDA content 3	OSDA content 4	OSDA content 2	OSDA content 3	OSDA content 4	OSDA content 2	OSDA content 3	OSDA content 4	OSDA content 2	OSDA content 3	OSDA content 4
	water content			%H			%C			%SDA		
TMDP (50%) + Imidaz (50%):												
0.110	42	43	45	2.0	2.3	2.6	3.8	5.6	7.2	5.4	7.9	10.2
0.080	30	31	31	1.7	2.0	2.4	4.0	5.8	7.5	5.6	8.1	10.5
0.070	26	26	27	1.6	1.9	2.3	4.0	5.8	7.5	5.6	8.2	10.6

water weight loss	OSDA content 2	OSDA content 3	OSDA content 4	OSDA content 2	OSDA content 3	OSDA content 4	OSDA content 2	OSDA content 3	OSDA content 4	OSDA content 2	OSDA content 3	OSDA content 4
	water content			%H			%C			%SDA		
TMDP (50%) + DMDP (50%):												
0.110	63	75	86	2.5	3.0	3.5	3.6	5.2	6.6	5.1	7.3	9.3
0.080	50	62	73	2.2	2.8	3.2	3.7	5.3	6.8	5.3	7.5	9.6
0.070	46	58	69	2.1	2.7	3.2	3.8	5.4	6.8	5.4	7.6	9.7

References

1. M. M. Mohamed, T. M. Salama, I. Othman and I. A. Ellah, *Micropor. Mesopor. Mater.*, 2005, **84**, 84–96.
2. B. O. Hincapie, L. J. Garces, Q. Zhang, A. Sacco and S. L. Suib, *Micropor. Mesopor. Mater.*, 2004, **67**, 19–26.
3. B. Han, S.-H. Lee, C.-H. Shin, P. A. Cox and S. B. Hong, *Chem. Mater.*, 2005, **17**, 477–486.
4. S.-H. Lee, C.-H. Shin, D.-K. Yang, S.-D. Ahn, I.-S. Nam and S. B. Hong, *Micropor. Mesopor. Mater.*, 2004, **68**, 97–104.
5. J. D. Gale, *J. Chem. Soc. Faraday Trans.*, 1997, **93**, 629–637.
6. J. D. Gale and A. L. Rohl, *Mol. Simul.*, 2003, **29**, 291–341.
7. C. G. Broyden, *J. Appl. Math.*, 1970, **6**, 222–231.
8. R. Fletcher, *Comput. J.*, 1970, **13**, 317–322.
9. D. Goldfarb, *Math. Comput.*, 1970, **24**, 23–26.
10. D. F. Shanno, *Math. Comput.*, 1970, **24**, 647–656.
11. A. K. Rappe and W. A. Goddard, *J. Phys. Chem.*, 1991, **95**, 3358–3363.
12. G. Sastre, S. Leiva, M. J. Sabater, I. Gimenez, F. Rey, S. Valencia and A. Corma, *J. Phys. Chem. B*, 2003, **107**, 5432–5440.
13. Y. G. Bushuev and G. Sastre, J. Phys. Chem. C, 2011, **115**, 21942-21953.
14. Y. G. Bushuev, G. Sastre and J. V. De Julián-Ortiz, J. Phys. Chem. C, 2010, **114**, 345-356.
15. Y. G. Bushuev and G. Sastre, Micropor. Mesopor. Mater., 2010, **129**, 42-53